AD 258 205

STEVENS INSTITUTE OF TECHNOLOGY
DAVIDSON LABORATORY
CASTLE POINT STATION
HOBOKEN, NEW JERSEY

QUARTERLY PROGRESS REPORT OCTOBER - DECEMBER 1960

RESEARCH PROGRAM ON CONVERSION OF EXPLOSIVE ENERGY

Contract DA-28-017-501-ORD-3450
DL Project LB-2221

Prepared by: S J Lukasik
S.J. Lukasik, Head
Fluid Physics Division

TABLE OF CONTENTS

Quarterly Progress Report October - December 1960
Research Program on Conversion of Explosive Energy

Contract DA-28-017-501-ORD-3450
DL Project LB-2221

SCOPE OF WORK

The work during the past quarter has been directed toward two main objectives, viz. compression of a magnetic field by a detonation and clarification of the importance of various secondary effects in the electrical conductivity measurements. In addition, some design work was performed relating to the 20,000 joule capacitor bank and the design of a large vacuum system in which to carry out firings.

The magnetic field compression experiments continued using the interim 1000 joule bank described earlier. The circuit parameters of this system were investigated in some detail in order to calculate the magnetic field in the load prior to its explosive compression. The signals induced in the pick-up loop during the firing were then analyzed in terms of a simple model picturing a constant total flux trapped in an area that is decreasing due to the expansion of the copper-clad explosive. A preliminary calculation of the leakage of the magnetic field into the conductors indicates that this effect is present though not a dominant feature of the experiment. Timing difficulties have still prevented crowbarring the bank at a current maximum despite several attempts to improve the timing accuracy. One of these attempts, involving a slower, high inductance, multi-turn coil, was unsuccessful due to mechanical failure of the coil. The most successful compression observed so far has been from an initial field of 4700 gauss to a final field of 38,500 gauss, or by a factor of 8.2. Efforts to obtain higher magnetic fields by redesigning the load coil and explosive "piston" and by working toward a higher initial magnetic field are continuing. The capacitors for the 20,000 joule bank ordered at the end of the last quarter were received at the end of the quarter reported on here. Most design work during the interim was suspended pending arrival of these units.

The conductivity work has been directed toward removing possible secondary effects in the conductivity measurements. These include the confinement of the detonation and consequent changes in the reaction zone

due to the structure supporting the double probes and the T-probes, the effect of the T-probe plate thickness, the difference between internal and surface conductivity measurements, and air-shock induced conductivity. Also, a faster sweep was employed in order to be able to examine the leading edge structure and the first half microsecond of the conductivity signal. On the basis of these firings, a revised set of measured conductivity values are reported that show better agreement with those of other investigators. Final values cannot be definitely established until all of the probe calibration data are reduced. General studies relating to the conductivity probe calibration have continued also. A summary of the double probe calibration procedure is attached as an appendix.

The final design of the large vacuum system was completed and construction proceeded during this quarter.

RESULTS OF WORK

A. Firings Conducted

During the past quarter, twenty eight firings have been conducted. These are listed in Table I. Four have been related to the magnetic field compression experiment while the remaining twenty four have involved electrical conductivity measurements.

B. Magnetic Field Work

The discrepancy between previous measurements of the bank and load inductances has been resolved. Ringing frequency measurements with and without the field coil yielded the following values for inductance and resistance:

$$L_{bank} = 102.5 \pm 3.5 \text{ m}\mu\text{h},$$

$$L_{system} = 175.5 \pm 9.2 \text{ m}\mu\text{h},$$

$$R_{bank} = .0342 \pm .0034 \ \Omega \approx R_{system}$$

Hence $$L_{coil} = 73 \pm 9.8 \text{ m}\mu\text{h}.$$

In the Quarterly Progress Report of Oct. - Dec. 1959, it was theoretically shown, for field coils of the present geometry, that the field in the center of the coil is given by the expression

$$B = 188 \times 10^{-7} i,$$

where i is the instantaneous current flowing in the field coil. Since B is proportional to voltage in the air gap,

$$B(r) = \frac{B(0)}{V(0)} V(r).$$

In the Quarterly Progress Report of April - June 1960, the radial dependence of the z-component of the magnetic field is shown. In particular, $V(0) = 3.30$ mv. Hence

$$B(r) = \frac{188 \times 10^{-7} i}{3.30} V(r),$$

where $V(r)$ is in mv and $B(r)$ is in gauss. Now

TABLE I

Firing No.	P.A. No.	Date	Type Charge	Camera Coverage	Purpose
93	1-1073	7 Oct.	Comp B cast in copper tube	none	magnetic field compression
94	1-1074	11	"	"	" " "
95	1-1080	20	"	streak	radial expansion velocity
96	1-1081	21	"	"	magnetic field compression

Conductivity Firing No.	Date	Explosive	Type Probe	Probe Location	Atmosphere	Confinement
22-c	2 Dec.	Pentolite	T	surface	Propane	confined
23-c	6	Comp B	double	"	Air	"
24-c		"	T	"	Propane	"
25-c		"	"	"	"	"
26-c	9	"	double	"	"	unconfined
27-c	27	"	"	"	"	"
28-c	28	"	"	"	"	confined
29-c		"	"	"	"	"
30-c	3 Jan.'61	"	"	"	"	unconfined
31-c		Comp B + 1% $CsClO_4$	"	"	"	"
32-c	4	Pentolite	"	"	"	"
33-c		"	"	"	"	"
34-c	9	Comp B	"	"	"	"
35-c		Comp B + 1% $CsClO_4$	"	"	"	"

TABLE I

Firing No.	P.A. No.	Date	Type Charge	Camera Coverage	Purpose
93	1-1073	7 Oct.	Comp B cast in copper tube	none	magnetic field compression
94	1-1074	11	"	"	" " "
95	1-1080	20	"	streak	radial expansion velocity
96	1-1081	21	"	"	magnetic field compression

Conductivity Firing No.	Date	Explosive	Type Probe	Probe Location	Atmosphere	Confinement
22-c	2 Dec.	Pentolite	T	surface	Propane	confined
23-c	6	Comp B	double	"	Air	"
24-c		"	T	"	Propane	"
25-c		"	"	"	"	"
26-c	9	"	double	"	"	unconfined
27-c	27	"	"	"	"	"
28-c	28	"	"	"	"	confined
29-c		"	"	"	"	"
30-c	3 Jan.'61	"	"	"	"	unconfined
31-c		Comp B + 1% $CsClO_4$	"	"	"	"
32-c	4	Pentolite	"	"	"	"
33-c		"	"	"	"	"
34-c	9	Comp B	"	"	"	"
35-c		Comp B + 1% $CsClO_4$	"	"	"	"

TABLE I (continued)

Conductivity Firing No.	Date	Explosive	Type Probe	Probe Location	Atmosphere	Confinement
36-c	10 Jan.	Comp B + 1% KNO_3	double	surface	Propane	unconfined
37-c		Comp B	T	"	"	minimum confinement
38-c	11	"	double	internal	--	--
39-c		"	"	"	--	--
40-c		"	"	"	--	--
41-c	12	"	T	surface	Propane	minimum confinement
42-c		"	"	"	"	" "
43-c		"	"	"	"	" "
44-c	13	"	"	"	"	" "
45-c		"	"	"	"	" "

$$\phi_{coil} = L_{coil} i = \int_{\text{air gap}} \bar{B} \cdot d\bar{A}$$

$$= \int_0^{2\pi} \int_0^{r_o} B(r)\, r\, dr\, d\theta = 2\pi \int_0^{r_o} B(r)\, r\, dr$$

$$= 2\pi \frac{188 \times 10^{-7} i}{3.30} \int_0^{r_o} V(r)\, r\, dr,$$

where r_o is the radius of the air gap. Hence

$$L_{coil} = \frac{2 \quad 188 \times 10^{-7}}{3.30} \int_0^{r_o} V(r)\, r\, dr.$$

By carrying out the indicated integration graphically, it is found that

$$L_{coil} = 87.8\ m\mu h,$$

in reasonably good agreement with the experimentally determined value.

Four more firings, Nos. 93-96, were completed in this quarter. In these firings a small notch was made in the upper part of the air gap of the field coil, in order to further protect the pickup coil from the explosive products and thus prolong its life. Also eight turns of aluminum foil were wrapped tightly around the copper-lined charge so that the expanding metallic surface would remain a closed conducting path for a longer period of time. Timing difficulties resulted in firings 93 and 94 crowbarring 9 μ secs late and firing 96 crowbarring 1.5 μ secs late. The oscilloscope trace of the pickup coil voltage as a function of time for firing No. 96 is shown in Fig. 1. The voltage is directly proportional to the magnetic field. Crowbarring was planned to occur at point A, the maximum uncompressed field, but timing errors resulted in crowbarring at point B, close to the minimum field. The magnetic field was then compressed to point C, and it is believed that the coil broke up at point D. If crowbarring had occurred at point A (19,500 gauss), the compression ratio of 8.2 would have resulted in a final field of 160,000 gauss instead of 38,500 gauss. The results of these firings are shown in Table II.

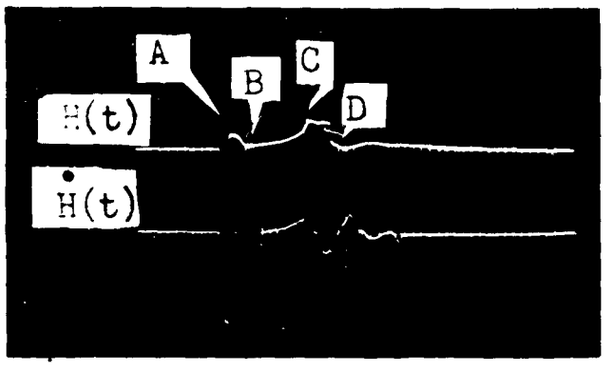

Figure 1

Oscilloscope trace showing the magnetic field as a function of time during a flux compression. The horizontal time scale is 5μsec/cm (Firing No. 96)

Table II

Summary of Magnetic Field Compression Firings

Firing No.	$B_{crowbar}$ (gauss)	B_{final} (gauss)	Compression Ratio
93	6,460	23,160	3.6
94	3,260	3,994	1.2
95	streak camera coverage only		
96	4,700	38,500	8.2

where the compression ratio is $B_{final}/B_{crowbar}$.

In firing No. 95, the streak camera results yielded information on the position and velocity of the copper sheath lining the charge as a function of time. Using this information, theoretical values for the magnetic field can be found, both considering and neglecting magnetic field penetration into the conductors. It is of interest to compare these calculations with the experimental values.

If no magnetic flux penetrates the conductors,

$$B(t) = \text{Constant} \left[\frac{1}{A(t)} \right] = \frac{\phi_{crowbar}}{A(t)} \qquad (1)$$

where $\phi_{crowbar}$ is the magnetic flux at crowbar ($t = 0$) and $A(t)$ is the time-dependent area of the air gap. $\phi_{crowbar}$ is easily found to be 1.35×10^{-3} w, yielding $B(0) = 5,870$ gauss. To compare with experimental values, for which $B(0) = 4,700$ gauss, the theoretical values are normalized so that they agree with the experimental values at $t = 0$.

Assuming magnetic flux penetration into the conductors, Maxwell's equations can be shown to yield the following relation if the displacement current is negligible

$$\frac{d\phi(t)}{dt} = \int \frac{\partial \bar{B}}{\partial t} \cdot d\bar{A} - \oint (\bar{v} \times \bar{B}) \cdot d\bar{l} \quad ,$$

where the first integral extends across the air gap, and the second integral is made around the conducting surface. Then $d\phi(t)/dt$ can be numerically integrated to obtain $\phi_{crowbar} - \phi(t)$. Then $B(t)$ is given by

$$B(t) = \frac{\phi(t)}{A(t)} = \frac{1}{A(t)} \left[\phi_{crowbar} + (\phi(t) - \phi_{crowbar}) \right] . \qquad (2)$$

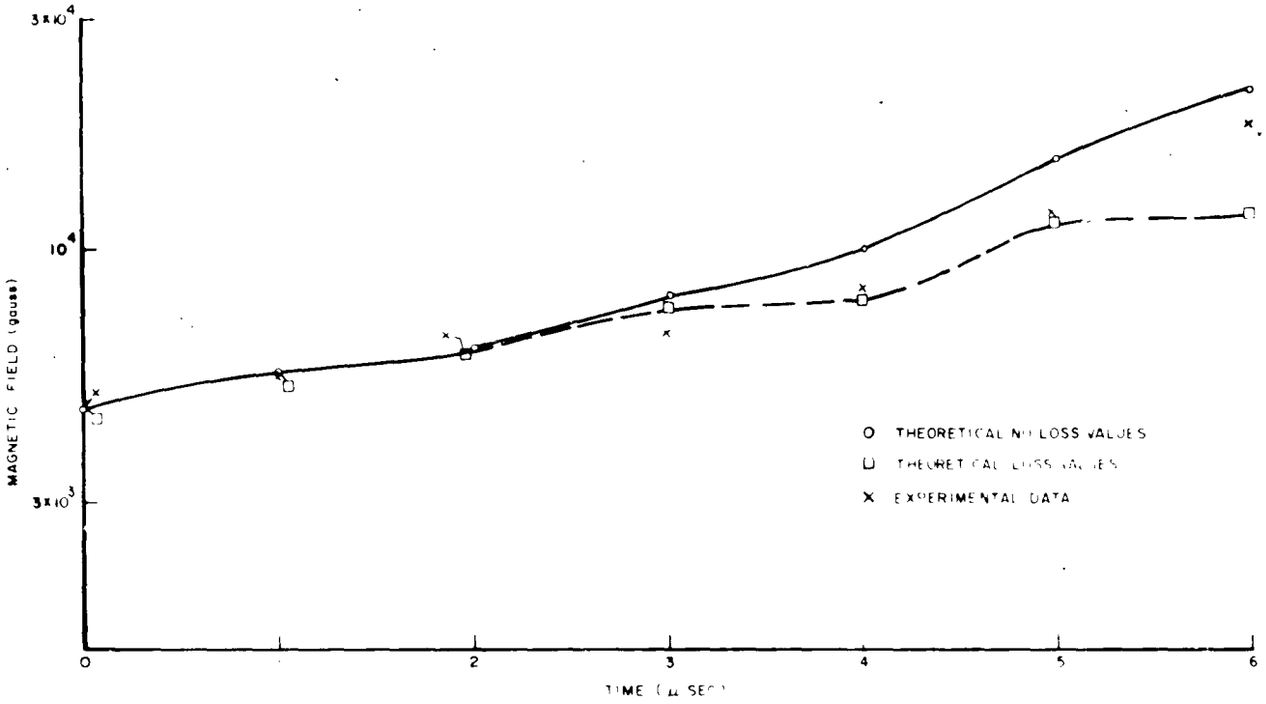

Figure 2

Magnetic field compression vs. time

Figure 2 shows the experimental and theoretical values for $B(t)$. The upper curve, marked by circles, represents the magnetic field as a function of time assuming that no flux penetrates the conductors (eq. 1). The lower curve, marked by squares, shows the magnetic field as a function of time calculated from eq. (2) assuming flux leakage into the conductors. It is based on measured values for $\dot{B}_{\theta}$ and $A(t)$. The experimental values obtained from the pick-up loop are shown by x's. These points generally lie between the two theoretical curves; it is believed that the discrepancy between the experimental points and the theoretical loss points is due to the uncertainties involved in calculating the above two integrals.

C. Conductivity Measurement

Firings 22-c through 45-c utilized surface double probes, internal double probes, and T probes for conductivity measurements in Composition B and Pentolite under varying experimental conditions. Table III summarizes the results of these firings.

The double probes are calibrated with a fixed input voltage of 0.1 volt, for varying salt solution depths and a single input pulse in a manner similar to that described in the July - Sept. 1960 Quarterly Progress Report. The choice of an input voltage of 0.1 volt for calibration purposes is based on the observed saturation of probe resistance with input voltage, as shown in Fig. 2 of the above report.

To provide a check on the validity of the single pulse calibration technique, a T probe, in a salt solution of known dimensions, was calibrated in a similar fashion to a double probe. The T probe resistance, calculated from the geometry and NaCl solution conductivity is 40.0 ohms. The resistance, as determined from the data of the pulse calibration is 37.9 ohms; this value corresponds to an extrapolated resistance for zero input pulse duration. This gives one confidence in the essential correctness of the single pulse calibration technique. It provides no information, however, on the correctness of using an electrolytic solution to calibrate a probe to be used to measure the electrical resistance of a detonation. This will be the subject of further investigation.

Figure 3(a) shows an assembly for measuring surface resistance; the probe is located on top of a rectangular charge and is held in place by

Table III

Double Probe Firing No.	Explosive	Probe Location	Probe Voltage	Atmosphere	Confinement	Initial Resistance (ohms)	Resistivity (ohm cm)	
23-c	Comp B	Surface	12v	Air	confined	6.11	0.66	average*
26-c	"	"	"	Propane	unconfined	--	--	no record
27-c	"	"	"	"	"	12.58	1.36	average* cracked probe
28-c	"	"	"	"	confined	6.07	0.63	average*
29-c	"	"	"	"	"	--	--	poor record
30-c	"	"	"	"	unconfined	5.06	0.39	incomplete+
32-c	Pentolite	"	"	"	"	10.08	0.84	average*
33-c	"	"	"	"	"	11.28	1.13	incomplete+
34-c	Comp B	"	0	"	"	--	--	zero probe voltage
31-c	Comp B + 1% $CsClO_4$	"	12	"	"	15.55	1.0	slow trace only
35-c	"	"	"	"	"	12.20	0.47	incomplete+
36-c	Comp B + 1% KIO_3	"	"	"	"	9.95	0.83	incomplete+
38-c	Comp B	Internal	"	--	--	--	--	poor record
39-c	"	"	"	--	--	7.81	0.93	average*
40-c	"	"	85	--	--	8.67	0.92	incomplete+

* Average resistivity corresponding to the spread in probe calibration

\+ Incomplete probe calibration data

Table III (continued)

T Probe

Firing No.	Explosive (inch)	Confinement	Atmosphere	Resistance (ohms)	Resistivity (ohm cm) probe thickness (variable)	Resistivity (ohm cm) reaction zone thickness (0.25 mm)	
22-c	Pentolite (2x2x4)	confined	Propane	23.06	1.15	0.58	slow sweep
24-c	Comp B (1x2x4)	"	"	22.28	2.23	1.11	" "
25-c	" "	"	"	34.28	3.43	1.71	" "
37-c	" "	minimum confinement	"	6.30	3.68	0.32	fast sweep
41-c	" "	"	"	5.95	0.57	0.30	" "
42-c	" "	"	"	5.95	0.45	0.30	" "
43-c	" "	"	"	13.85	0.56	0.69	" "
44-c	" "	"	"	8.63	0.22	0.43	" "
45-c	" "	"	"	8.84	0.04	0.44	" "

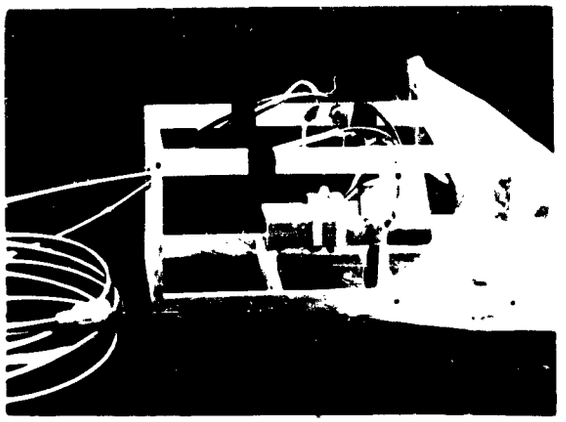

Figure 3(a)

Surface-mounted double probe

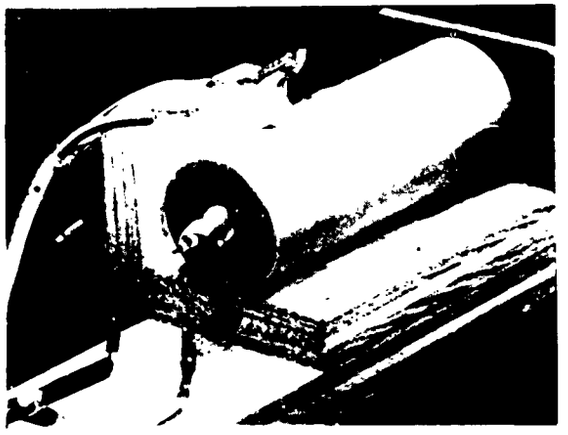

Figure 3(b)

Internally-mounted double probe

mounting it in a polyethylene block. The oscilloscope trigger probes are positioned between the explosive and the detonator which is located at the right. The wooden frame and plastic bag provide for carrying out the measurement in a propane atmosphere. To reduce explosive confinement due to the polyethylene block supporting the double probe in later firings some of the polyethylene material was removed in the vicinity of the probe tip. The probe support then resembles a table, the legs of which mount on the surface of the explosive block. The probe is supported by pressing the conical base against the polyethylene "table top".

A typical oscilloscope record in Fig. 4(a) illustrates the rapid onset of conduction as the detonation front reaches the probes. Since the physical condition of the probe is uncertain at later times, only the probe resistance corresponding to the initial peak was computed. Both traces are for the same event, but for different sweep rates. The upper trace shows a 20 μsec time history of the detonation while the lower trace shows a 2 μsec interval that includes the leading edge of the signal.

Figure 3(b) shows an assembly used for internal resistance measurements. A double probe can be seen extending from the exposed face of the explosive. Oscilloscope trigger probes are shown leading to the surface. The detonator is located behind the rear support. Figure 4(b) shows a typical oscilloscope record. Comparing this with Fig. 4(a) we see that they both show a peak conduction at 5 shakes but that the later time history of the event differs. Our interpretation is that this peak represents reaction zone conduction while the remainder of the trace refers to conduction by reaction products.

T probe assemblies with varying copper plate thicknesses have also been fired. In order to minimize confinement, much of the polyethylene support holding the thin copper plate has been cut away with just enough left to insulate the sides of the copper plate and maintain its rigidity when pressed against the explosive block. Such a mounting is shown in Fig. 5. The dependence of the probe resistance on probe thickness is shown in Fig. 6.

The reaction zone length at the surface of the explosive can be estimated by observing the variation of measured explosive resistance with T probe thickness. For large probe thicknesses the conduction path is determined by the width of the reaction zone, whereas for a small probe

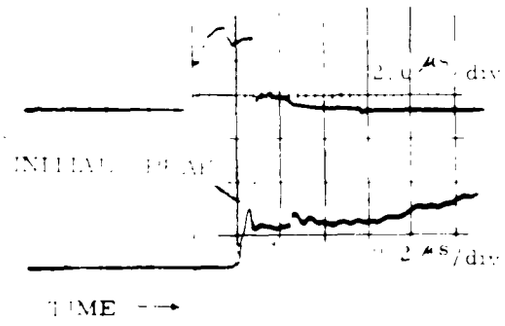

Figure 4(a)

Oscilloscope trace for surface-mounted

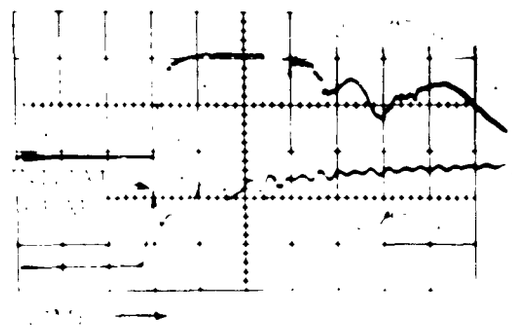

Figure 4(b)

Oscilloscope trace for internally-

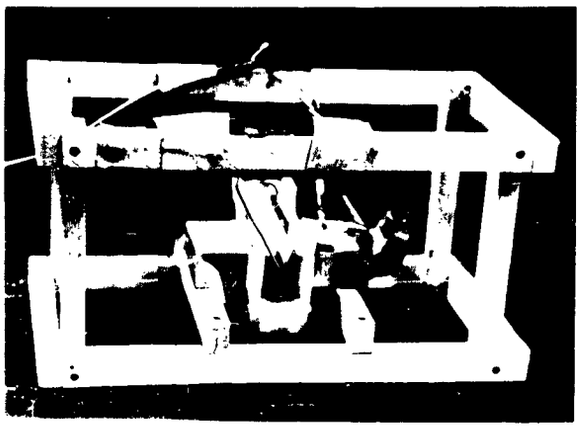

Figure 5

T probe mounted on surface of charge

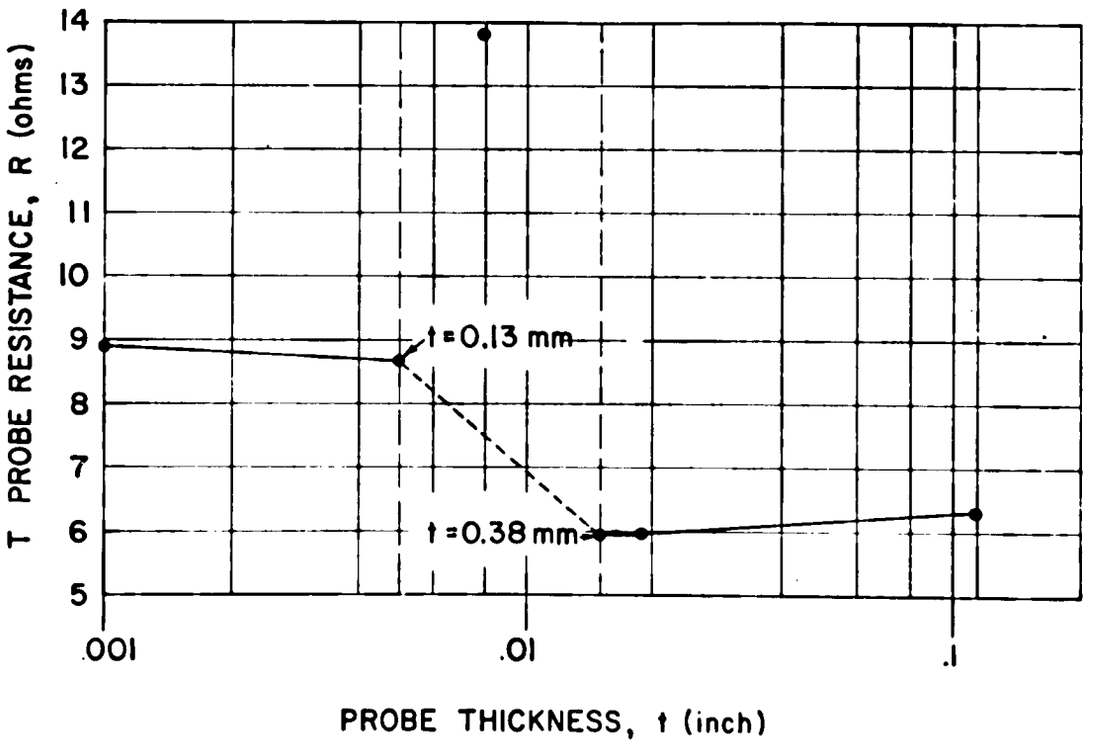

Figure 6

thickness the conduction path depends strongly upon probe thickness. The transition between 0.13 and 0.38 mm is believed to be indicative of the reaction zone length in Comp B.

Comparison of the explosive resistivity values that have been obtained under various experimental conditions is shown below in Table IV. Two contaminating factors are inherent in surface measurements, air-shock induced conductivity and confinement of the detonation. The variations due to confinement are outstanding, 0.66 vs 0.39 ohm-cm for the unconfined case, whereas attempts to inhibit air shock contributions by using a propane atmosphere yielded no significant difference, 0.66 vs 0.63 ohm-cm. Internal measurements, free of air shock and confinement effects, are indicative of the extent to which shock-induced conduction can modify surface results, comparing the values 0.39 with 0.92 ohm-cm.

Table IV

Comparison of Explosive Resistivity Under Various Conditions

Explosive	Resistivity (ohm cm)	Probe location	Atmosphere	Confinement
Comp B	0.66	surface	air	confined
	0.63	surface	propane	confined
	0.39	surface	propane	unconfined
	0.92	internal	NA	unconfined
Pentolite	0.99	surface	propane	unconfined
Comp B + 1% $CsClO_4$	0.47	surface	propane	unconfined
Comp B + 1% KNO_3	0.83	surface	propane	unconfined

The addition of an easily-ionized material has not apparently increased the conductivity. Preliminary measurements with 1% $CsClO_4$ and KNO_3 have been made and firings with higher concentrations are underway. The resistivity values observed for Pentolite are roughly twice those for Comp B.

Both the magnitude of the resistivity and difference between Comp B and Pentolite are substantially in agreement with similar measurements of other investigators as shown below in Table V. Comparison of surface resistivities with results from BRL show a close correspondence. The factor of 2.5 discrepancy for internal resistivity values with University of Utah results is believed to be attributable to calibration uncertainties in the latter measurements.

Table V

Comparison of Measured Explosive Resistivity (ohm cm)

surface	BRL[1]	Stevens	Utah[2]	LASL[3]	Soviet[4]
Comp B	0.29	0.39	--	--	0.2
Pentolite	0.89	0.99	--	--	--
internal					
Comp B	--	0.92	2.56	0.24 at 0.5 μs 0.056 at 0.08 μs	--

WORK PLANNED FOR NEXT QUARTER

During the next quarter the design and most of the construction of the large capacitor bank is expected to be completed. This will include the connection of the line to the capacitor, the transmission line, and the spark gap switch, as well as the overall structure.

The conductivity work will be largely directed toward analyzing the present results. In particular the circuit rise time will be examined and the effect of cable delay will be determined. This is important since the present minimum resistivity values are based on an initial current maximum, the height of which may be critically dependent on the circuit parameters.

In an attempt to increase explosive conductivities work with seeded explosives will continue. Composition B charges with 10% $CsClO_4$ and KNO_3 are being fabricated. A small quantity of CsI has been obtained and similar seeding concentrations in Composition B will be started as soon as compatability tests are completed.

To improve the magnetic field compressional efficiency, a tear drop coil has been designed. Plastic standoffs have been placed so that crowbarring will occur very soon after detonation, thus minimizing the amount of flux escaping before the crowbar time. The size of the air gap has been decreased so that the copper sheath does not expand beyond 75% of its initial radius before the gap is closed. This is done to lessen the possibility of the copper surface rupturing before the gap is closed. The coil also has a slightly higher inductance to lessen timing errors. In order to further improve the compression ratio, ways of optimizing the pickup coil position and decreasing its overall size are being studied. This effectively increases the ratio of initial crowbarred area of the air gap to the area of the pickup coil. For the tear-drop design and the present pickup coils, this ratio is about 10/1.

REFERENCES

(1) R.L. Jameson "Electrical Measurements in Detonating Pentolite and Composition B" 3rd Symposium on Detonation, Princeton Univ., Sept. 1960, pg 120.

(2) M.A. Cooke, R.T. Keyes, L.D. Lee, E.F. Pound "Measurements of Ionization and Electron Densities in the Detonation Wave of Solid Explosives" Tech. Rep. No. 1, Explosives Research Group, Univ. of Utah, Sept. 15, 1956.

(3) B. Hayes "On the Electrical Conductivity of Detonating High Explosives" 3rd Symposium on Detonation, Princeton Univ., Sept. 1960, pg 139.

(4) A.A. Birsk, M.S. Tarasov, V.A. Tsukerman "The Electrical Conductivity of the Products of an Explosion of Condensed Explosives" JETP, 37, 1095 (1959).

PERSONNEL

Personnel of Stevens Institute of Technology who have been associated with the work reported here are:

Dr. W.H. Bostick
Dr. S. Koslov
Dr. S.J. Lukasik
Mr. H.J. Pernick
Mr. L.H. Weeks

Personnel of Picatinny Arsenal who have contributed to the project are:

Dr. J.V.R. Kaufmann
Dr. E.H. Clark
Mr. F. Schwartz
Mr. I. Kintish
Mr. E. Walbrecht
Mr. I. Dalrymple

APPENDIX

Double Probe Calibration Technique

When probe geometry and configuration result in a complicated current density distribution, calibration of the probe is necessary to establish the numerical relation between measured resistance and resistivity. For a pair of electrodes immersed in a medium of resistivity ρ, one has

$$\rho = \text{const.} \times R \tag{1}$$

where R is the measured resistance corresponding to ρ. Thus, in calibrating a particular probe, one is concerned with obtaining the numerical value of the constant factor for that probe. If the probe resistance for a material of known resistivity is measured then:

$$\frac{\rho_c}{R_c} = \text{const.}$$

and hence

$$\rho = \frac{\rho_c}{R_c} R$$

where ρ_c is the known resistivity and R_c is the measured resistance corresponding to ρ_c.

A double probe, consisting of two adjacent lengths of wire separated and surrounded by an insulator, with exposed metallic tips, must be calibrated in order to compute explosive resistivity from the observed probe resistance during detonation. The exposed probe tip is immersed into a solution of NaCl of known conductivity and the probe resistance is measured under various operating conditions. The ratio ρ_c/R_c is determined from these measurements.

Due to electrolytic action in the NaCl solution and the generation of gas bubbles that adhere to the probe surface thus drastically changing the current density distribution across the surface and the probe resistance, a method of resistance measurement that minimizes this source of error must be employed. Use of a DC technique is ruled out due to the constant rate of gas production and excessively large resistance values

observed. Use of an AC method reduces somewhat the amount of gas formation about the electrodes and simultaneously the measured resistance but since the probe impedance is now frequency-dependent, one must use a very high frequency driving source or extrapolate low frequency results to infinite frequency. A third technique is to use a pulsed electrical driving source, whose pulse duration is adjusted so that gas bubble corruption of the measured probe resistance is substantially reduced. An extension of this method is to use a single pulse generator, thus reducing buildup of gas bubbles due to repetitive electrical pulsing of the probes.

Description of Calibration Apparatus and Procedure

The double probe to be calibrated is connected in series with a decade resistance box to a single pulse generator, as shown in Fig. 7. A dual beam oscilloscope displays the output voltage of the generator and the voltage across the probe simultaneously. The oscilloscope sweep is initiated by means of a trigger pulse from the single pulse generator that precedes in time the single pulse applied to the probes. The time duration and amplitude of the single pulse to the probes are variable parameters.

Prior to calibration a probe is inspected for breaks and cracks in the ceramic insulator; the exposed tips are lightly scraped with fine emery paper to remove any unwanted polyester material and to have the wire tips and ceramic edge flush. An ohmmeter is then used to check that the probe is not shorted before being placed into a conducting solution. A large current, (obtained by setting the pulse generator controls to a maximum voltage output and a maximum repetitive duty cycle), is then passed through the probes immersed in a conducting solution until bubble formation is observed. The probe leads are then reversed and the procedure repeated. This step is intended to leave the probe tips electrically clean.

The probe is then placed into a bath of a freshly prepared, filtered, NaCl solution with only the probe tip being wetted by the salt solution; the bath shape conforming to the geometry of the explosive charge. The depth of the salt solution in the bath is varied during the calibration, to detect effects of solution depth upon calibration. To minimize bubble formation, even with a single pulse calibration scheme, a voltage about which the probe resistance shows little variation is chosen. Since the salt solution conductivity is temperature dependent, the solution temperature

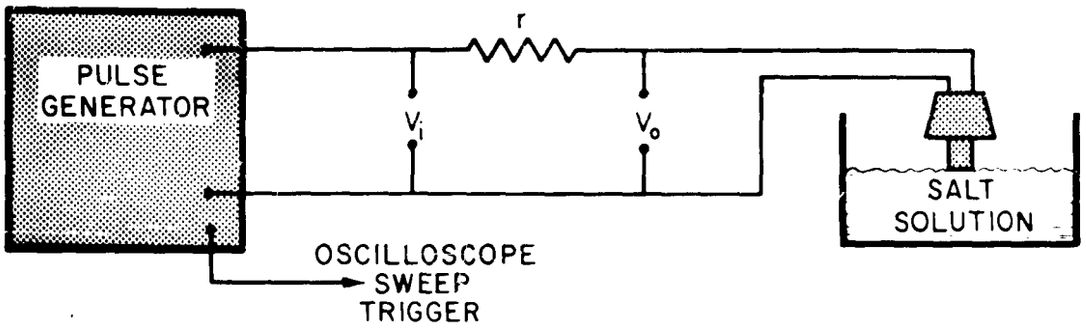

Figure 7

Circuit for double probe calibration

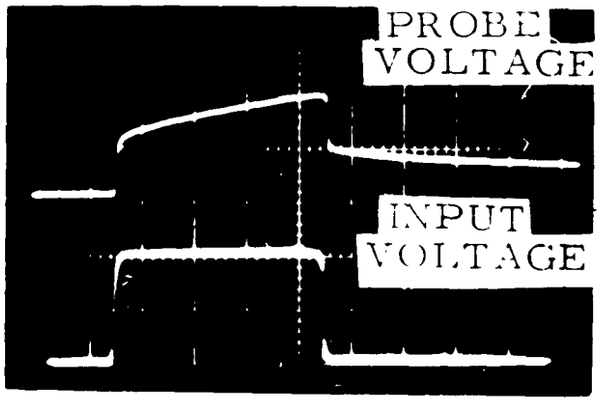

is recorded through the calibration procedure. The probe is then calibrated under varying input pulse durations by manually operating the single pulse generator and photographing the voltage wave forms displayed on the oscilloscope screen. Typical calibration parameters are: input pulse duration of 1, 5, and 10 μ sec, solution depths of 0.047, 0.072, and 0.125 in. and an input pulse voltage of 0.1 volt. Thus, for each probe a total of nine runs are obtained. A typical record of these wave forms is shown in Fig. 8, the lower trace refers to the generator output voltage and the upper trace to the probe output voltage.

After calibration the probe is washed with distilled water to remove remaining traces of salt.

The probe resistance is calculated from data derived from the photographic records. To facilitate data reduction, the oscilloscope photographs are enlarged to a convenient size, about five times magnification. The probe resistance is calculated from the result (derived later) that

$$R_c = \frac{r\,V_o(\tau_1)\,A_o(\tau_2) - r\,V_o(\tau_2)\,A_o(\tau_1)}{V_o(\tau_1)\left|A_i(\tau_2) - A_o(\tau_2)\right| - V_o(\tau_2)\left|A_i(\tau_1) - A_o(\tau_1)\right|} \qquad (2)$$

where R_c = probe resistance in NaCl solution

r = fixed resistance in calibration circuit

$V_o(\tau_1)$, $V_o(\tau_2)$ = probe voltage at an arbitrarily chosen time τ_1, τ_2 respectively

and where $A_o(\tau) = \int_o^{\tau} V_o(t)\,dt$

and $A_i(\tau) = \int_o^{\tau} V_i(t)\,dt$,

$V_i(t)$ = the generator voltage curve.

The necessary time, voltage, and area values are obtained from an oscilloscope record enlargement, areas being measured by a planimeter. The data are then prepared and arranged for digital computer processing and computation. The computer has been programmed to calculate in addition

to probe resistance, the probe capacitance and estimated r.m.s. errors in resistance and capacitance.

Derivation of Equation (1)

Consider a pair of electrodes immersed in a medium of conductivity σ as illustrated below. The current density $\bar{J}$ and electric field $\bar{E}$ are related by

$$\bar{J} = \sigma \bar{E}$$

An external emf maintains a potential V across the probe electrodes; the series current through the probes and battery is I.

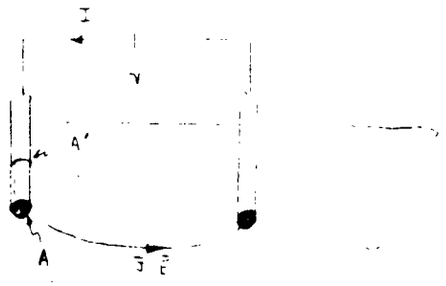

Integrating the above relation across the conduction tip area A (shaded area in the above figure) gives

$$\int_A \bar{J} \cdot d\bar{A} = \sigma \int_A \bar{E} \cdot d\bar{A} = I = \frac{V}{R}$$

where R is the probe resistance. Thus

$$R = \frac{V}{\sigma \int_A \bar{E} \cdot d\bar{A}} \quad . \tag{2}$$

The integral can be readily evaluated by the following consideration. Consider a closed Gaussian Area A_G consisting of the conduction area A and a section of the probe A' so that $A_G = A + A'$ encompasses a closed volume. The area A' lies just inside of the probe surface along the cylindrical edges. Thus, from Gauss' law, in the absence of the conducting medium,

$$\int_{A_G} \bar{E}\, d\bar{A} = \frac{CV}{\epsilon_o} \qquad (4)$$

where C is the probe capacity. Then

$$\int_{A_G} \bar{E}\cdot d\bar{A} = \int_{A} \bar{E}\cdot d\bar{A} + \int_{A'} \bar{E}\cdot d\bar{A} = \int_{A} \bar{E}\cdot d\bar{A}$$

Since $\bar{E} = 0$ across A', i.e. the electrostatic field inside a conductor vanishes we have

$$\int_{A} \bar{E}\cdot d\bar{A} = \frac{CV}{\epsilon_o}$$

The integrals, $\int_A \bar{E}\, dA$ appearing in Eqs. (3) and (4) are identical, since the field $\bar{E}$ is derivable in both cases from a scalar potential ψ, where

$$\nabla^2 \psi = 0,$$

with identical boundary conditions in both situations. Hence

$$\epsilon = \frac{\epsilon_o}{C}$$

Thus, for a given probe geometry and configuration one has

$$k' = k/\rho = \text{const.}$$

and, if k_c, ρ_c refer to calibration values, then

$$\rho = \frac{\rho_c}{k_c} k \quad .$$

Derivation of Equation (2)

The calibration circuitry can be represented schematically as:

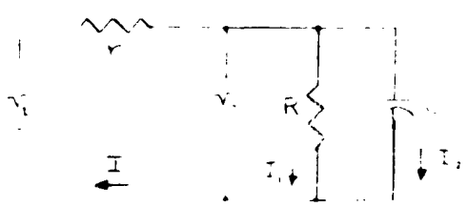

where R, C represent the probe resistance and capacity, r is the fixed series resistance, V_i is the generator voltage, and V_o is the probe voltage. One has

$$V_i = Ir + I_1 R = Ir + q_2/C \tag{5}$$

so that

$$I_1 = \frac{V_i - Ir}{R}$$

and also

$$I_2 = I - I_1$$

Differentiating eq. (5)

$$\frac{dV_i}{dt} = r\frac{dI}{dt} + \frac{I_2}{C} = r\frac{dI}{dt} + \frac{I}{C} - \frac{I_1}{C}$$

$$\frac{dV_i}{dt} = r\frac{dI}{dt} + \frac{I}{C} - \frac{1}{C}\,\frac{V_i - Ir}{R}$$

Hence

$$\frac{dV_i}{dt} + \frac{V_i}{RC} = r\frac{dI}{dt} + \left(\frac{R+r}{RC}\right)I$$

Now

$$V_o = V_i - Ir$$

so that

$$I = \frac{V_i - V_o}{r}$$

and

$$\frac{dV_i}{dt} + \frac{V_i}{RC} = \frac{dV_i}{dt} - \frac{dV_o}{dt} + \left(\frac{R+r}{RrC}\right)(V_i - V_o)$$

or

$$\frac{V_i}{RC} - \left(\frac{R+r}{RrC}\right)V_i = -\frac{dV_o}{dt} - \left(\frac{R+r}{RrC}\right)V_o$$

Thus

$$\frac{V_i}{rC} = \frac{dV_o}{dt} + \left(\frac{R+r}{RrC}\right) V_o \quad .$$

Integrating from $t = 0$ to $t = \tau$

$$\frac{1}{rC} \int_o^\tau V_i dt = V_o(\tau) - V_o(0) + \left(\frac{R+r}{RrC}\right) \int_o^\tau V_o \, dt \quad .$$

Define

$$A_i(\tau) = \int_o^\tau V_i \, dt$$

$$A_o(\tau) = \int_o^\tau V_o \, dt$$

and set $V_o(0) = 0$.

Then

$$\frac{1}{rC} A_i(\tau) = V_o(\tau) + \left(\frac{R+r}{RrC}\right) A_o(\tau)$$

$$\therefore A_i(\tau) = RrC \, V_o(\tau) + (R+r) A_o(\tau) \quad .$$

Hence

$$\frac{R\left[A_i(\tau) - A_o(\tau)\right] - r A_o(\tau)}{Rr \, V_o(\tau)} = C$$

Evaluating the left hand side at $\tau = \tau_1$ and τ_2

$$\frac{R\left[A_i(\tau_1) - A_o(\tau_1)\right] - r A_o(\tau_1)}{V_o(\tau_1)} = \frac{R\left[A_i(\tau_2) - A_o(\tau_2)\right] - r A_o(\tau_2)}{V_o(\tau_2)}$$

Solving for R

$$R = \frac{r \, V_o(\tau_1) A_o(\tau_2) - r \, V_o(\tau_2) A_o(\tau_1)}{V_o(\tau_1)\left[A_i(\tau_2) - A_o(\tau_2)\right] - V_o(\tau_2)\left[A_i(\tau_1) - A_o(\tau_1)\right]}$$

Using this value for R, one can solve for C

$$C = \frac{R\left[A_i(\tau_1) - A_o(\tau_1)\right] - r\,A_o(\tau_1)}{Rr\,V_o(\tau_1)}$$

In addition, one can ascertain the root mean square error in R and C due to errors in the measured quantities, r, $V_o(\tau_1)$, etc., as follows. The error in R due to an error in any of the measured values can be written as

$$\Delta R_1 \simeq \frac{\partial R}{\partial r}\,\Delta r$$

$$\Delta R_2 \simeq \frac{\partial R}{\partial V_o(\tau_1)}\,\Delta V_o(\tau_1), \text{ etc.}$$

Thus one generates the following error terms for R

$$\Delta R_1 = R\,\frac{\Delta r}{r}$$

$$\Delta R_2 = \frac{A_o(\tau_2)\,(r+R) - A_i(\tau_2)R}{D}\,\Delta V_o(\tau_1)$$

$$\Delta R_3 = \frac{R\,A_i(\tau_1) - A_o(\tau_1)\,(R-r)}{D}\,\Delta V_o(\tau_2)$$

$$\Delta R_4 = \frac{(r+R)\,V_o(\tau_1)}{D}\,\Delta A_o(\tau_2)$$

$$\Delta R_5 = -\frac{(r+R)\,V_o(\tau_2)}{D}\,\Delta A_o(\tau_1)$$

$$\Delta R_6 = -\frac{R\,V_o(\tau_1)}{D}\,\Delta A_i(\tau_2)$$

$$\Delta R_7 = \frac{R\,V_o(\tau_2)}{D}\,\Delta A_i(\tau_1)$$

where

$$D = V_o(\tau_1)\left[A_i(\tau_2) - A_o(\tau_2)\right] - V_o(\tau_2)\left[A_i(\tau_1) - A_o(\tau_1)\right]$$

Likewise one has for the error terms in C

$$\Delta C_1 = -\left[\frac{A_i(\tau_1) - A_o(\tau_1)}{r\,V_o(\tau_1)} + \frac{A_o(\tau_1)}{R\,V_o(\tau_1)}\right]\frac{\Delta r}{r}$$

$$\Delta C_2 = -\left[\frac{C}{V_o(\tau_1)} + \frac{A_o(\tau_1)}{R^2 V_o(\tau_1)} \frac{A_o(\tau_2)\ (r+R) - A_i(\tau_2)\ R}{D}\right] \Delta V_o(\tau_1)$$

$$\Delta C_3 = -\frac{A_o(\tau_1)}{R^2 V_o(\tau_1)} \frac{R\ A_i(\tau_1) - A_o(\tau_1)\ (R-r)}{D}\ \Delta V_o(\tau_2)$$

$$\Delta C_4 = \left[\frac{1}{r\ V_o(\tau_1)} - \frac{A_o(\tau_1)}{R\ V_o(\tau_1)} \frac{V_o(\tau_2)}{D}\right] \Delta A_i(\tau_1)$$

$$\Delta C_5 = \frac{A_o(\tau_1)}{RD}\ \Delta A_i(\tau_2)$$

$$\Delta C_6 = \left[\frac{A_o(\tau_1)\ (r+R)\ V_o(\tau_2)}{R^2\ D\ V_o(\tau_1)} - \frac{R+r}{R\ r\ V_o(\tau_1)}\right] \Delta A_o(\tau_1)$$

$$\Delta C_7 = -\frac{A_o(\tau_1)}{R^2 V_o(\tau_1)}\ \frac{(r+R)\ V_o(\tau_1)}{D}\ \Delta A_o(\tau_2)$$

The fundamental errors are estimated as follows. Δr is a manufacturers specified accuracy of 0.5%. ΔV is an estimate of the accuracy with which the voltage pulse height can be read; typically $\Delta V/V$ is of the order of 5%. ΔA represents the repeatability of a planimeter area reading for a given area; typically $\Delta A/A$ is of the order of 5%. The root mean square errors in R and C are obtained from

$$(\Delta R)^2 = \frac{1}{7} \sum_{i=1}^{7} (\Delta R_i)^2$$

$$(\Delta C)^2 = \frac{1}{7} \sum_{i=1}^{7} (\Delta C_i)^2$$

For each set of probe calibration data, values of Δr, $\Delta V_o(\tau_1)$, etc., obtained from error estimates of the measured quantities r, $V_o(\tau_1)$, etc. are provided. The final result from the computer is thus a calculation of R, C, and the r.m.s. errors in R and C. A summary of results of this calibration procedure for the probes calibrated to date will be presented in a later report.

Tabulation of NaCl Solution Conductivity

The conductivity of a standard salt solution (an excess of NaCl in distilled water, about 450 grams per liter)*

$(ohm\ cm)^{-1}$	Temp. (^{o}C)
0.1345	0
0.1555	5
0.1779	10
0.2014	15
0.2062	16
0.2111	17
0.2160	18
0.2209	19
0.2259	20
0.2309	21
0.2360	22
0.2411	23
0.2462	24
0.2513	25
0.2565	26
0.2616	27
0.2669	28
0.2721	29
0.2774	30

*Values taken from "Handbook of Chemistry and Physics" 38th Edition, 1956-1957

DISTRIBUTION LIST

Commanding Officer
Diamond Ordnance Fuse Laboratories
Washington 25, D. C.

Technical Reference Section (1)

Commanding General
Aberdeen Proving Ground
Aberdeen, Maryland

BRL - Dr. R. Eichelberger (1)

Chief of Ordnance
Department of the Army
Washington 25, D. C.

ORDTB (1)

Armed Services Technical Information Agency
Arlington Hall Station
Arlington 12, Virginia (10)

Commanding Officer
Picatinny Arsenal
Dover, New Jersey

Purchasing Office, ORDBB-PB1 (5)

Commanding Officer
Office of Ordnance Research
Box CM, Duke Station
Durham, North Carolina

Dr. Sherwood Githen (1)

Explosives Research Laboratory
Bureau of Mines
4800 Forbes Avenue
Pittsburgh 13, Pennsylvania

Dr. F. Gibson (1)

Carnegie Institute of Technology
Pittsburgh, Pennsylvania

Dr. F. Allison (1)

Mr. Laddie L. Stahl
Manager - Technical Relations
General Electric Company
Schenectady, New York (1)

Dr. Arthur H. Guenther
Director, Pulse Power Laboratory
Air Force Special Weapons Center
Kirtland Air Force Base
New Mexico (1)

Dr. David Berstein
Poulter Laboratories
Stanford Research Institute
Menlo Park, California (1)